

***Modeling and Monitoring of Air Quality in Gulf
Cooperation Council (GCC) Capitals Using Satellite
Technology and GIS Based analysis***

Dr. Hany Rabie Nady ⁽¹⁾

Dr. Emad Abdelfattah Saleh Hafez ⁽²⁾

Abstract:

The nations of the Gulf Cooperation Council (GCC) are the most economically active in the world. Major cities and capitals have seen an influence on air quality due to the recent economic boom. There are over 59.7 million people living in the Gulf Cooperation Council nations, of which approximately 29.0 million are citizens and 30.7 million are immigrants. One of the most significant economic pillars in this region is oil production, coupled with other economic booms in the industries, tourism, and agriculture sectors. The current study predicts, monitors, and observes air quality in the capitals of the Gulf Cooperation Council (GCC) using Landsat-8 OLI and TIRS pictures, GIS tools, and other techniques. The main land covers were mapped using Landsat-8 images.

The aerosol optical thickness (AOT) and aerosol path radiance were computed using the exoatmospheric solar constant and atmospheric transmittance. The results, which rely on Landsat-8 OLI satellite monitoring of atmospheric gases, show notable variations in the concentrations of air contaminants. The study found that there were notable PM10 concentrations in Abu Dhabi and Doha when the air quality index increased to 100. The lowest air quality index score was 96 in Muscat City and the highest value was 162 in Abu Dhabi City. In Riyadh, Kuwait, Manama, and Doha, it was around (123-132- 130-154), correspondingly.

Keywords: Modeling, Monitoring, Air Quality, GCC.

(1) Lecturer of Geography, Faculty of Arts, Beni -Suef University.

(2) Lecturer of physical geography and geographic information systems at the Faculty of Arts, Beni-Suef University.

Introduction:

Air pollution, especially in metropolitan, is a serious public health concern. Since it negatively affects human health, survival, and activities as well as those of other living things. PM is a complex admixture of varying size, content, and concentration of both solid and liquid droplets and particles suspended in the air. PM₁₀ with a mass median aerodynamic diameter of less than 10 μm can travel up to 30 miles in one hour and remain in the atmosphere for minutes at a time. Particulate matter (PM) is emitted directly through a variety of natural processes, as well as from various anthropogenic activities, or is generated indirectly as a result of chemical reactions in the atmosphere. Aerosol is made up of liquid droplets and suspended, minute particulate matter (PM₁₀) with a diameter smaller than 10 microns. Aerosol optical thickness (AOT) and PM₁₀ mass concentration calculations are used to determine the amount of atmospheric turbidity caused by aerosols, which is regarded as a general indicator of air pollution. Climatologists and meteorologists believe that the nature of troposphere has begun to change and its balance is disturbed due to the increase of air pollutants volume. This confirms the emergence of a dense layer of pollutants appearing over the oceans and the Arctic. It can be said that the problem of air pollution is due to the exploitation and depletion of energy resources such as coal and nuclear energy and the increase of both industrial and population concentration in cities. More than 80% of individuals who live in metropolitan areas are exposed to air that is of lower quality than what the World Health Organization (WHO) advises. People who live in metropolitan areas may be more susceptible to health issues like asthma, chronic and acute respiratory disorders, heart disease, lung cancer, and stroke as the quality of the air in those locations deteriorates. In addition to evaluating the air quality in a specific region, ongoing monitoring and knowledge acquisition of air contaminants are necessary to comprehend and resolve a number of environmental challenges. (WHO). In this study, the concentration of air pollution over the (GCC) capitals was calculated using the AOT and PM₁₀ measurements collected by Landsat 8 (OLI_TIRS) following imaginary processing in the winter, summer, and fall of 2021.

2. Study Area:

The study area is located in western Asia, consisting of six capitals of the Gulf Cooperation Council countries represented in Riyadh, Kuwait, Manama, Doha, Abu Dhabi and Muscat, (Fig. 1). Due to the region's exposure to frequent dust storms, particularly in spring and summer, which load significant dust particles into the air and negatively impact human activities and cause air pollution, whether these pollutants are natural or anthropogenic have an impact on the (GCC) countries' air quality. On the other hand, the region is witnessing high growth rates in addition to excessive energy use, heavy traffic, water desalination plants, and industrial plants, all of which are significantly increasing anthropogenic aerosol emissions.

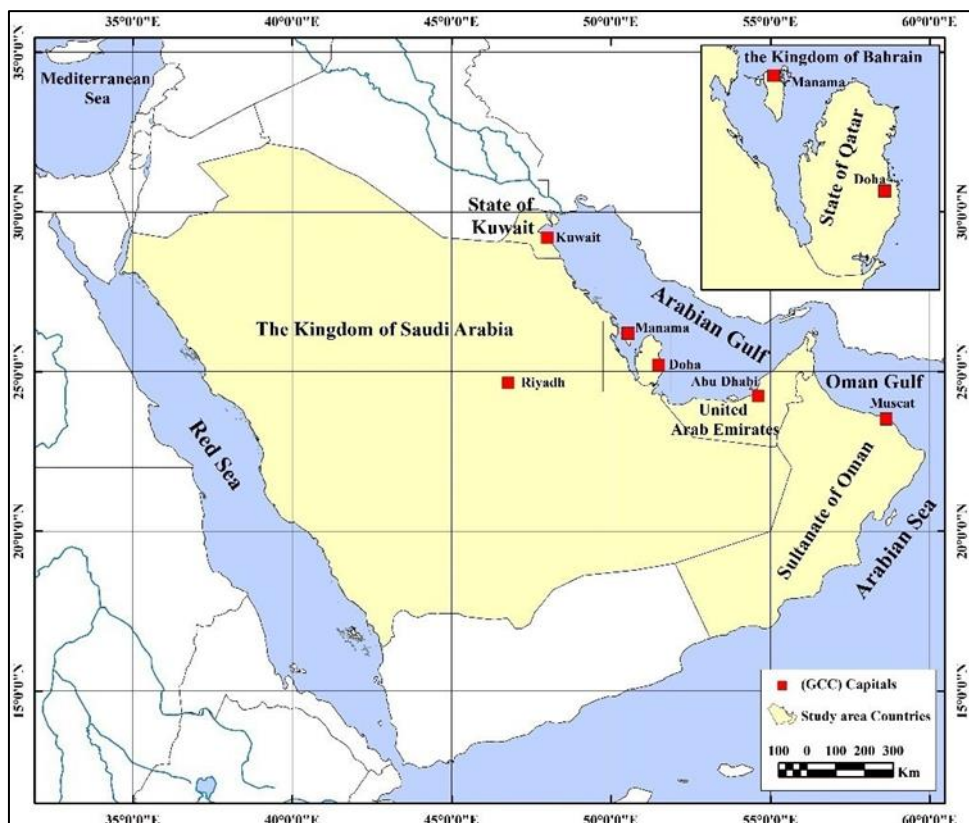


Fig. (1) (GCC) Countries location

Six cities that serve as the capitals of the (GCC) nations make up the study region (Figs. 2 and 3), which can be displayed as follows:

2.1. Riyadh: Riyadh is the capital of the kingdom of Saudi Arabia and is the largest city in area and population. It is also considered the Arabian

Peninsula largest city in population. The city is located in the eastern part of Najd plateau westward an-Nafud desert, as its surface slope grades from the northwest to the southeast. Riyadh is characterized with its hyper-arid region climate as the mean daily temperature is 26.6 and the mean humidity is 26% and annual precipitation is 94.6 (mm). North and northeastern winds are prevailing, its blow during summer and spring resulting dust and ash storms and therefore in the increase in PM10. Population of Riyadh reached 10.5 million people with 29.7% of the kingdom population, with population density of 4659 persons/km², as population concentrate in city center districts which represent the city core and northern districts. Whereas, industrial activities concentrate in the south of the city, therefore pollution rats increase in this part of the city. Residential areas cover 38.2% of the city area, while vegetation covers 4.2% and deserts take 57.6 of the city area, (Fig. 3).

2.2. Kuwait: Kuwait City is the capital of the State of Kuwait and its largest cities in area and population. The attached determination of the city limits represents the combination of Kuwait, Holy, Farwaniya, Mubarak El Kabeer, Ahmady and Gahraa. The area of all these cities is about 855.9 km² populated by about 74.8 % of entire country population. Residential areas are the dominant land cover for the city as it covers about 85% of the city area followed by desert areas with 9.8%, then vegetation cover with 5.1% and water bodies with 0.1%. Kuwait City has many air polluting activities represented in the numerous industrial areas like Shuwaikh, Doha, Amghrah, Sabhan, Saleebyah and El Shabeyah. In addition to petroleum refining activities and pollutants resulting from car exhaust – as the number of cars exceeded 2.3 million cars, and other air pollutant human activities.

2.3. Manama: Manama is the capital of the Kingdom of Bahrain and its largest cities in area and population. The city is located in the northeastern part of the Kingdome of Bahrain westward Meharaq island with an area of 23.8 Km² and population over 0.5 million people and population density of 6835 person/Km². Residential areas cover 83.6% of the city area followed by vegetation 10.9%, then deserts areas with 5.1% and water bodies with 0.4% of the city areas. Air pollutants industrial activities are mainly in the southern part of the city where the Salman harbor industrial area.

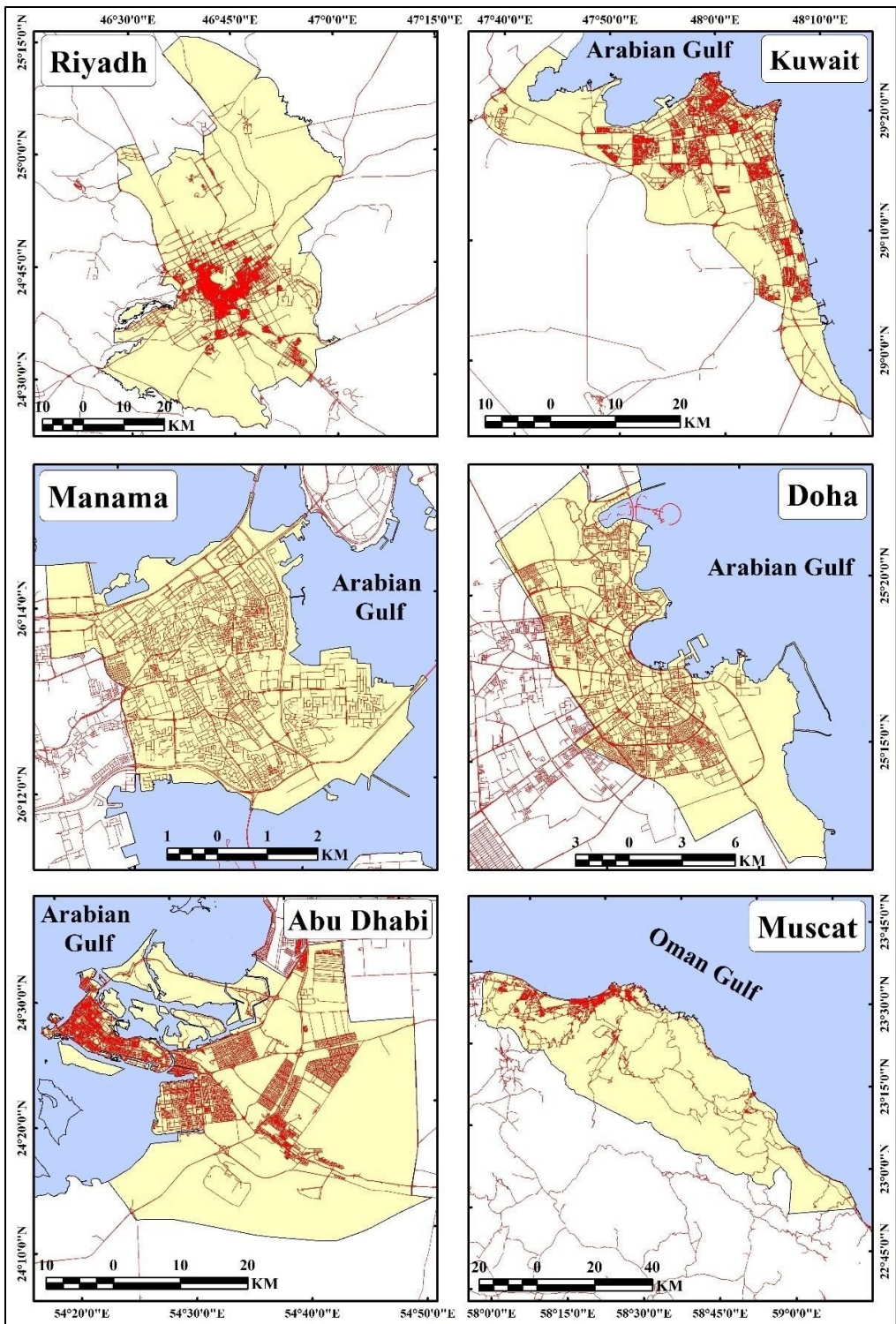


Fig. (2) GCC capitals location

2.4. Doha: Doha, capital of Qatar and its largest cities in area and population. It is 155.5 Km² with over 0.65 million people. Population density reaches 4191 person/Km². Doha is located in the eastern coast of Qatar, in the middle part of the country, which affected its air quality and made it rank second of PM₁₀ concentration in the GCC countries. Residential areas are prevailing land cover with 84.1% of the city area, followed by vegetation which cover 9.7%, then desert with 5.9% and water bodies 0.3% of the city area. High population density concentrates in middle and north parts, while industrial activities concentrate in south and west parts.

2.5. Abu Dhabi: the capital of the United Arab Emirates, which is located on an island in the Arabian Gulf, it is 1548.5 Km² with over 1.5 million people with mean population density of 1000 person/Km². Desert lands cover about 47% of the city area, which are the future development areas and represent one of the city's main sources of air pollution. Whereas Residential areas cover 40.8% of the city area, as urban concentrate in Abu Dhabi Island and new expansions on Abu Dhabi coast. Vegetation cover 10.6% and water bodies 1.6% of the city area.

2.6. Muscat: Muscat is the capital of Sultanate of Oman and its largest cities in area and population, with an area of 3654.7 Km² while its population are 1.6 million people with 30.8% of the Sultanate population and 355 person/Km² density. Muscat Governorate combines Muscat, Muttrah, Al Seeb, Al Amarat, Bawshar and Qurayyat province. Mountain and desert areas cover 78.1% of its area representing a source of dust storms blown toward the city with the burst of sandstorm. Residential areas cover 19.0% of the city area, and are centered in coastal area and decrease in density westwardly at the mountain edge. Northwards there are more residential areas, whereas southwards there are less. Vegetation covers 2.8%, and water 0.1% of the city area.

3. Research data and methods:

Data collecting, data pre-processing, and data processing are the three main categories into which the research data and procedures can be classified.

3.1. Data acquisition:

In this study, Landsat-8 images were used to determine the seasonal changes of pollution concentrations in the capitals of the (GCC) (Table 1). the satellite imagery downloaded from (USGS), and in this study, AOT and PM10 were calculated using data from 24 Landsat-8 OLI images. Using supervised classification, the Landsat-8 images OLI sensor was used to map the major land covers (Fig. 3). It is noted that Landsat-8 images did not cover the entire area of the cities of Riyadh, Kuwait and Muscat, as it covered (94.7 - 96.7 - 83.7%), respectively. The missing parts of the three cities are the southeast of Riyadh, to the southeast of Al- Aziziyah Al-Janubiyah, Al-Bariyah and Khashm Al-Aan district, north- east of Kuwait, north-east of Al-Jahra Governorate, and southeast of Muscat, south of the province of Qurayyat.

Table 1 image specifications for Landsat-8 (OLI_TIRS)

Capitals	Path/Row	Winter			Spring			Summer			Autumn		
		Acquisition Date	Acquisition Time (AM)	Cloudiness	Acquisition Date	Acquisition Time (AM)	Cloudiness	Acquisition Date	Acquisition Time (AM)	Cloudiness	Acquisition Date	Acquisition Time (AM)	Cloudiness
Riyadh	166/43	23-Jan	07:23	0.53	13-Apr	07:23	10.18	02-Jul	07:23	0	22-Oct	07:24	0.01
Kuwait	165/40	16-Jan	07:16	2.35	06-Apr	07:16	0.17	25-Jun	07:16	0	15-Oct	07:16	0.01
Manama	163/42	18-Jan	07:04	2.12	08-Apr	07:04	0.1	27-Jun	07:04	0	01-Oct	07:05	0
Doha	163/42	18-Jan	07:04	2.12	08-Apr	07:04	0.1	27-Jun	07:04	0	01-Oct	07:05	0
Abu Dhabi	160/43	13-Jan	06:46	2.74	03-Apr	06:46	0.01	22-Jun	06:46	0	12-Oct	06:46	0
Muscat	158/44	29-Jan	06:34	5.77	02-Apr	06:34	0	24-Jun	06:34	0	14-Oct	06:35	0

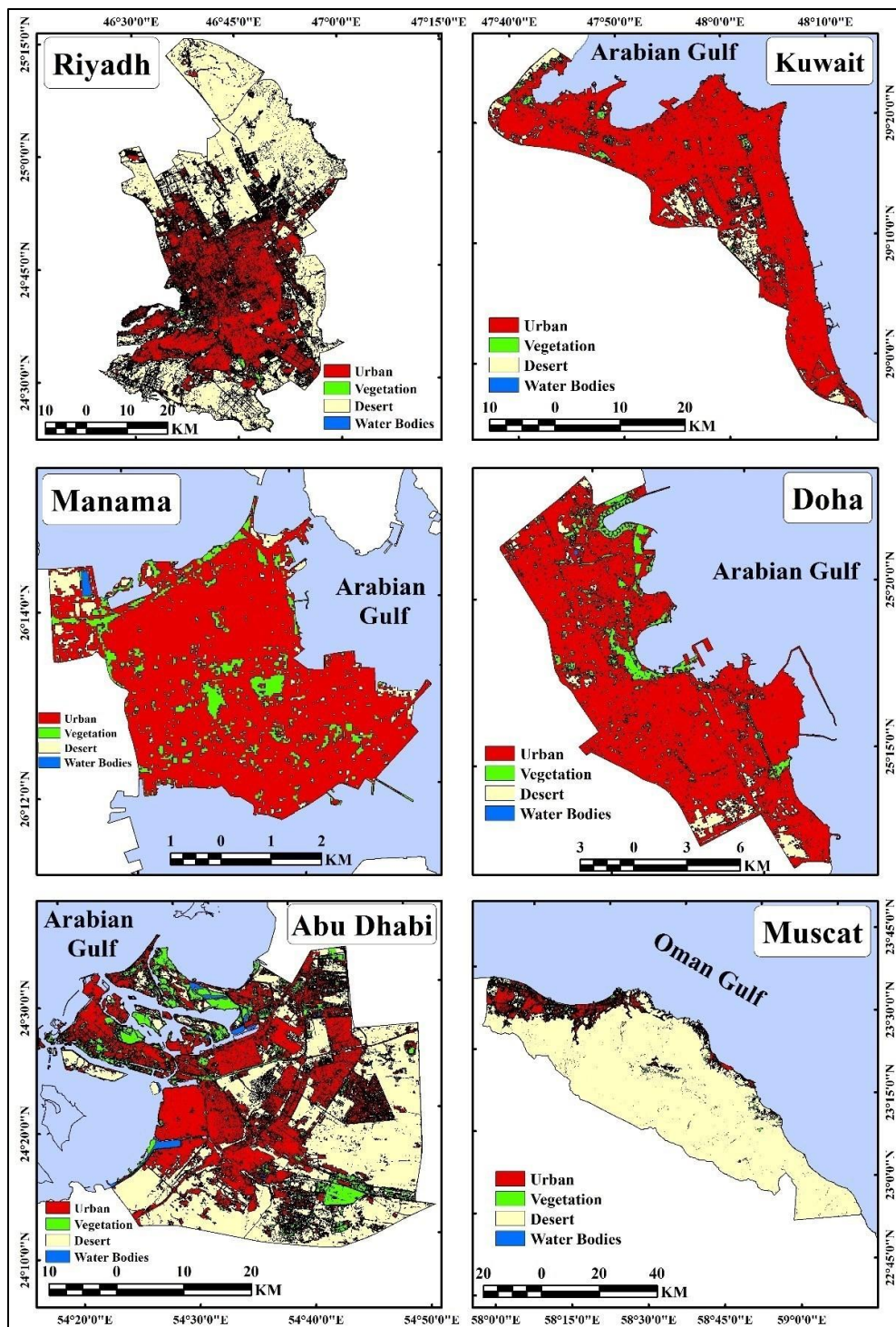


Fig. (3) GCC capitals Land use Land cover

3.2. Data preprocessing:

3.2.1. Conversion to TOA Radiance:

By using equation (1), (Nguyen, 2014), TOA spectral radiance was calculated from the radiance rescaling factors in the MTL file as follow:

$$L_{\lambda} = ML * Q_{cal} + AL \quad (1)$$

where: L_{λ} = TOA spectral radiance. M_L = Multiplying rescaling factor for a given band. A_L = additive rescaling factor for bands. Q_{cal} = pixel values of a standard product that have been quantized and calibrated (DN).

3.2.2. Conversion to TOA Reflectance:

using equation (2) for radiometric calibration of satellite images and equation (3) for a correction for the sun angle of TOA reflectance, (Sikder, 2018):

$$\rho\lambda' = M\rho * Q_{cal} + A\rho \quad (2)$$

$$\rho\lambda = \rho\lambda' / \cos(\theta SZ) = \rho\lambda' / \sin(\theta SE) \quad (3)$$

Where, $\rho\lambda$ = TOA planetary reflectance; $\rho\lambda'$ = TOA Solar angle-unadjusted planetary reflectance $M\rho$ = multiplicative rescaling factor for band $A\rho$ = additive rescaling factor for band Q_{cal} = Standard product pixel values that quantized and calibrated (DN); θSE = angle of local sun elevation; θSZ = Local solar zenith angle and $\theta SZ = 90^{\circ} - \theta SE$. Dark Object Subtraction (DOS 1) method is used to atmospheric correction.

3.2.3. Atmospheric Correction:

Band-specific rescaling factors are included in Landsat 8 images, enabling a simple conversion from DN to TOA. When measuring the reflectance at the ground, the effects of the atmosphere should be taken into account. the reflectivity of the land surface (ρ) is:

$$\rho = (\pi * L_{\lambda} * d^2) / (E_{sun\lambda} * \cos\theta) \quad (\text{Moran et al, 1992}) \quad (4)$$

Where, ρ = planetary reflectance L_{λ} = Spectral Radiance d^2 = Earth-Sun Distance $E_{sun\lambda}$ = Mean Solar Exoatmospheric Irradiances θ = Solar Zenith Angle in Degrees.

3.3. Data processing:

At this point, data from Landsat 8 (OLI_TIRS) images of the capitals of the GCC countries will be retrieved for both Aerosol Optical

Thickness (AOT) and particulate matter with a mass median aerodynamic diameter 10 m (PM10) values.

3.3.1. AOT Calculation:

To calculate the atmospheric reflectance, the amount given by the surface reflectance was subtracted from the reflectance obtained from the satellite (TOA) after radiometric correction. Calculate AOT based on such information using the method provided by (Nadzri, 2010):

$$\begin{aligned} AOT(\lambda) &= a_o R(\lambda) \quad (5) \\ R(\lambda) &= \rho a(\theta_{SZ}, \theta_v, \Phi) \\ a_o &= 4\mu\mu_o / \omega_o * \rho a(\theta_{SZ}, \theta_v, \Phi) \end{aligned}$$

Where, $R(\lambda)$ = atmospheric reflectance $\rho a(\theta_{SZ}, \theta_v, \Phi)$ = aerosol scattering phase function; θ_{SZ} = Local solar zenith angle; θ_v = Viewing zenith angle; Φ = Relative azimuth angles; μ = Cosines of the view directions; μ_o = Cosines of the illumination directions and ω_o = single scattering albedo.

3.3.2. PM10 Calculation:

Finally, using Eq (6), the mass concentration of PM10 was estimated, (Retails& Sifakis, 2010) as:

$$PM_{10} = 195.7 \tau_a + 14.5 \quad (6)$$

where, τ_a is Aerosol Optical Thickness (AOT). Figures 5-6-7-8-9-10 and Table 2 both display the calculated PM10 concentration in the capital cities of the Gulf Cooperation Council. To generate the mean yearly air quality map presented in (Table 3) and (Fig. 11), the PM10 concentration map was averaged.

4. Results and discussion:

4.1. PM10 concentration (Mean, Maximum and Minimum):

4.1.1. Mean annual concentration of PM10:

PM10 mean annual concentration ranged between 92.4 $\mu\text{g}/\text{m}^3$ in summer and 86.0 $\mu\text{g}/\text{m}^3$ in winter, while it's concentration in spring and autumn was 90.5-91.0 $\mu\text{g}/\text{m}^3$, respectively (Table 2) and (Fig. 4). The high summer, autumn and spring concentration of PM10 is associated with the prevailing climatic conditions, where the high temperature, wind activity towards low pressure and the activity of dust and sand storms, which increases its concentration in the air. While its concentration decreases in winter with the stability of weather conditions and the decrease in temperature.

4.1.2. Maximum annual PM10 concentration:

The maximum annual concentration of PM10 ranged between 406.3 $\mu\text{g}/\text{m}^3$ in winter and 259.3 $\mu\text{g}/\text{m}^3$ in autumn, while its concentration in spring and summer was 287.3-259.3 $\mu\text{g}/\text{m}^3$, respectively. The high winter and autumn concentration of PM10 is due to the passage of cells of low pressure that cross the Mediterranean Sea and southern Europe through the northern part of the Arabian Peninsula in the winter, in addition to local cells of low pressure due to local heating on sunny days, which leads to the movement of air quickly and speed up air movement in a spiral around those cells, thus stirring up dirt and dust. On certain winter days, the slow wind speed caused elevated pollution concentrations near to the earth's surface.

4.1.3. Minimum annual PM10 concentration:

The minimum annual concentration of PM10 ranged between 48.7 $\mu\text{g}/\text{m}^3$ in autumn and 40.7 $\mu\text{g}/\text{m}^3$ in winter, while in spring and summer was 44.1-47.0 $\mu\text{g}/\text{m}^3$, respectively. This is due to the high temperature and wind activity.

Table 2 Mean, Maximum and Minimum concentration of PM10 in GCC capitals 2021

capitals	Winter				Spring				Summer				Autumn			
	Max.	Min.	Mean	Std.	Max.	Min.	Mean	Std.	Max.	Min.	Mean	Std.	Max.	Min.	Mean	Std.
Riyadh	639.3	39.5	82.6	12.7	235	47.8	86.6	11.4	274	39.7	85.1	12.5	283	41.7	85.4	12.4
Kuwait	342.9	56.2	88.6	9.3	597	44.1	86.1	10.1	488.3	37.6	94.1	12.8	692.9	52.2	88.8	10.1
Manama	141.3	57	84.9	10.5	153.4	63.7	92.7	10.2	168.1	56.4	90.2	11.1	156.8	51.2	85.9	12.2
Doha	209.5	57.6	97.9	14.4	273.2	52.4	103.9	16.2	199.8	56.5	100.6	12.9	222.6	52.1	101.6	16.6
Abu Dhabi	875.1	2.4	96.7	17.9	233.2	23.4	101.9	15.1	214.1	49.7	105.9	13.8	278.1	39.4	115	22.6
Muscat	229.5	31.5	65.5	12.5	232.2	33.4	71.6	11.5	211.3	42	78.8	10	642.7	55.7	69.3	13.2

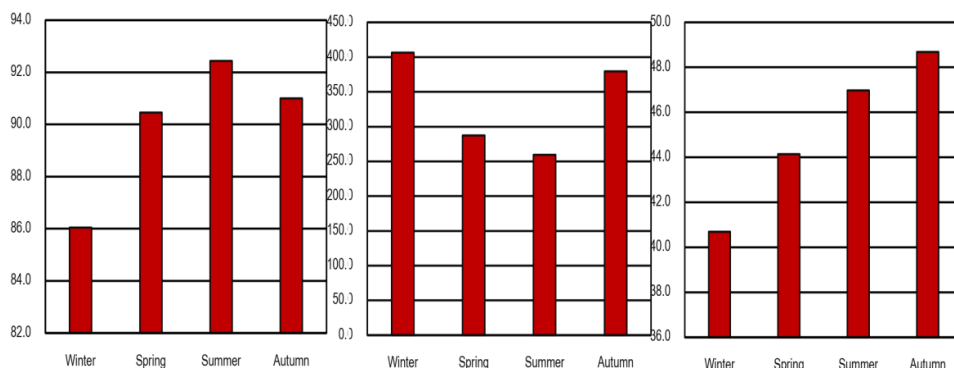


Fig. (4) Mean, Maximum and Minimum PM10 in GCC capitals

4.2. PM10 concentration in (GCC) capitals:

4.2.1. Riyadh: PM10 mean annual concentration in Riyadh was 84.93 $\mu\text{g}/\text{m}^3$, ranging from 86.57 $\mu\text{g}/\text{m}^3$ in spring to 82.64 $\mu\text{g}/\text{m}^3$ in winter. It also ranged between 357.83 $\mu\text{g}/\text{m}^3$ as a maximum value and 42.16 as a minimum value. Riyadh is PM10 mean annual concentration reveals that 94.37% of the city is Moderate (50–100 $\mu\text{g}/\text{m}^3$ year). Other parts of the city ranges from unhealthy for sensitive groups (100–150 $\mu\text{g}/\text{m}^3$ year) 5.22%, to very unhealthy categories (200 -300 $\mu\text{g}/\text{m}^3$ year) 0.38%, (Table2) and (Fig. 5). Areas with unhealthy air are distributed in the central and southern part of the city, where the district of Al-Sulay, Al-Mansuriya, and Al-Masha'el are all located near the industrial areas south the city like Aramco Riyadh refinery and new industrial city and Yamaha Saudi cement company. It is also noted that in winter high concentrations of pm10 have been observed in class of Hazardous (+300 $\mu\text{g}/\text{m}^3$ year) Which covers 0.01% of the city's area, which appeared in the northeastern part, where the areas of Al-Arja, Al-Raed, Hittin, Al-Rahmaniyah, and Al- Izdihar are areas with high development rates and a population density ranging from medium to high.

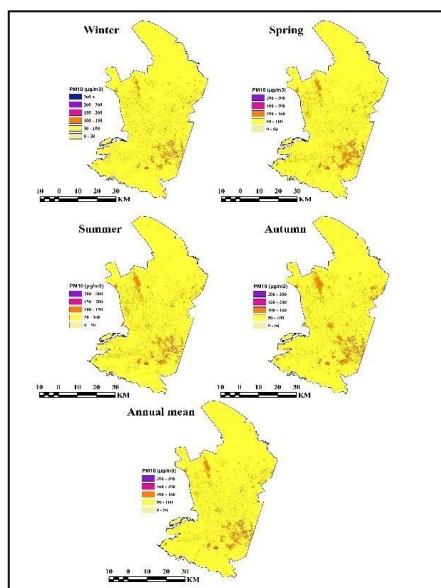


Fig. (5) Concentration of PM10 in Riyadh

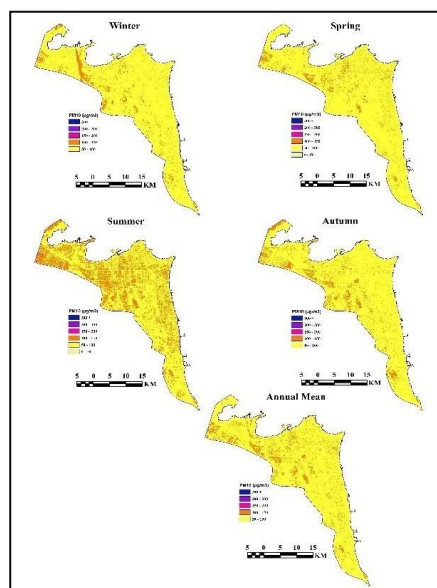


Fig. (6) Concentration of PM10 in Kuwait

4.2.2. Kuwait: The PM₁₀ concentration in Kuwait City as a mean annual is 89.39 $\mu\text{g}/\text{m}^3$, ranging from 94.12 $\mu\text{g}/\text{m}^3$ in Summer to 86.12 $\mu\text{g}/\text{m}^3$ in Spring, and ranged between 350.27 $\mu\text{g}/\text{m}^3$ as a maximum value and 47.51 as a minimum value. shows that PM₁₀ concentrations are high in Summer and spring, mean annual concentration of PM₁₀ in Kuwait reveals that 90.91% of the city is Moderate (50–100 $\mu\text{g}/\text{m}^3$ year) and 9.02% are unhealthy for sensitive groups (100–150 $\mu\text{g}/\text{m}^3$ year), other categories including unhealthy (150 -200 $\mu\text{g}/\text{m}^3$ year), very unhealthy (200 -300 $\mu\text{g}/\text{m}^3$ year) and Hazardous (+300 $\mu\text{g}/\text{m}^3$ year) cover about 0.07% of the city area (Fig. 6). It is also noted that the area occupied by the unhealthy for sensitive groups (100–150 $\mu\text{g}/\text{m}^3$ year) increased in the summer season to cover 25.4% of the city area affected by the prevailing climatic conditions and human activity, while the other three categories cover 0.1% of the city area. It is also clear from (Fig. 6) that areas with high concentrations of PM₁₀ are distributed in the central and western part of the city, specifically around industrial areas such as Shuwaikh and Sabhan industrial areas in the center, Amghara, Doha, Sulaibiya and Jahra industrial areas in the west and the Ahmadi industrial area in the south, along with some residential districts with high density, such as the district of Salwa, Bayan, Hawally and Al-Rai.

4.2.3. Manama: PM₁₀ mean annual concentration in Manama was 88.44 $\mu\text{g}/\text{m}^3$, which is higher than the annual limits allowed by (WHO), ranging between 92.73 $\mu\text{g}/\text{m}^3$ in spring and 84.93 $\mu\text{g}/\text{m}^3$ in winter, and also between 154.88 $\mu\text{g}/\text{m}^3$ as a maximum value and 57.08 as a minimum value. (Fig. 7) shows that the concentration of PM₁₀ in Manama ranges between two classes: Moderate (50–100 $\mu\text{g}/\text{m}^3$ year) class which cover 88.65% of the city area as a mean annual. Which exceeded that in winter and autumn seasons, reaching 92.02- 89.41 $\mu\text{g}/\text{m}^3$, respectively. The second class is unhealthy for sensitive groups (100–150 $\mu\text{g}/\text{m}^3$ year) which cover 11.35% of the city area as a mean annual, while this area increases to 17.63% in summer. Areas with high concentration of PM₁₀ are concentrated in the southeastern and southern parts, where the districts of Al-Qudaibah, Umm Al-Hassam, Al-Fateh, and Mina Salman industrial area are located, except that the

concentration of PM10 are in the class of Moderate concentration.

4.2.4. Doha: Doha comes as a second rank of PM10 concentration in (GCC) capitals, with a mean annual concentration of 100.98 $\mu\text{g}/\text{m}^3$, this placed it into the unhealthy for sensitive groups (100–150 $\mu\text{g}/\text{m}^3$ year). Although this average reached 103.87 $\mu\text{g}/\text{m}^3$ comes in the category of unhealthy for sensitive groups (100–150 $\mu\text{g}/\text{m}^3$ year) in spring with high temperature and dusty winds, and 101.58 $\mu\text{g}/\text{m}^3$ in autumn, it reached 97.8 $\mu\text{g}/\text{m}^3$ in winter. The annual mean ranged between 400.12 $\mu\text{g}/\text{m}^3$ as a maximum value and 28.71 $\mu\text{g}/\text{m}^3$ as a minimum. (Fig. 8) shows that the concentration of PM10 in Doha ranges between two classes Moderate (50– 100 $\mu\text{g}/\text{m}^3$ year) class which cover 50.64% of the city area as a mean annual, it exceeded that in winter reaching 60.36 $\mu\text{g}/\text{m}^3$. The second class is unhealthy (150 -200 $\mu\text{g}/\text{m}^3$ year) which cover 0.07% of the city area as a mean annual, while this area increases to 0.32% in Spring. The city has also reached a class of very unhealthy (200 -300 $\mu\text{g}/\text{m}^3$ year) in Spring, winter and autumn which cover (0.07-0.02-0.01%) respectively. In general, very unhealthy categories (200 -300 $\mu\text{g}/\text{m}^3$ year) concentrated in the eastern side of the city where the Hamad International Airport are located, and in the western side where industrial area are located.

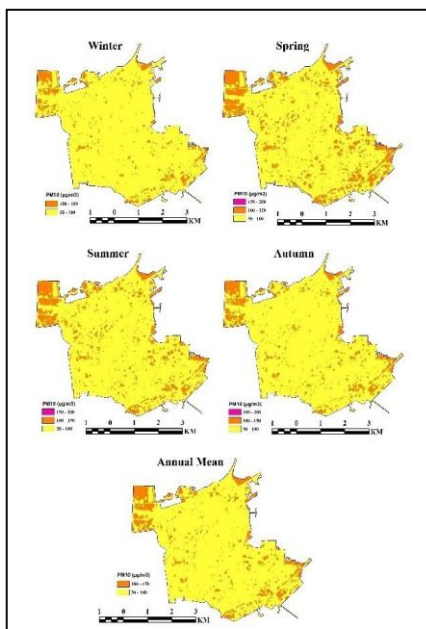


Fig. (7) Concentration of PM10 in Manama

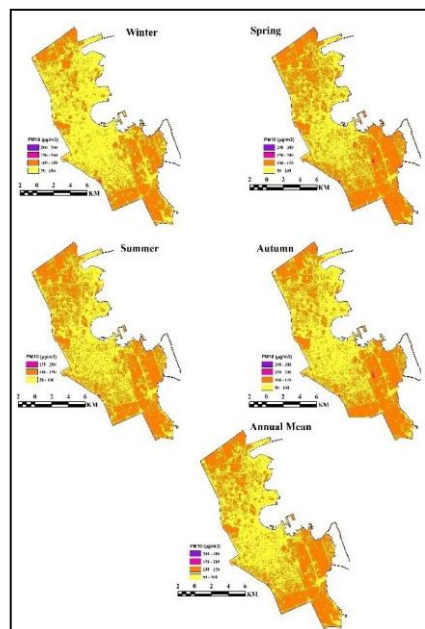


Fig. (8) Concentration of PM10 in Doha

4.2.5. Abu Dhabi: Abu Dhabi ranks first of the capitals of the GCC countries in PM10 high concentration, Where the annual average was $104.86 \mu\text{g}/\text{m}^3$, this placed it into the unhealthy air ($150 - 200 \mu\text{g}/\text{m}^3$ year), which reached a high level of pollution than (WHO) maximum limit for one year. this average increases to $114.99 \mu\text{g}/\text{m}^3$ in autumn and $105.86 \mu\text{g}/\text{m}^3$ in summer, while it recorded $96.73 \mu\text{g}/\text{m}^3$ in winter. Maximum annual concentration of PM10 is $400.12 \mu\text{g}/\text{m}^3$, therefore it ranked at Hazardous air quality ($+300 \mu\text{g}/\text{m}^3$ year). While minimum annual concentration of PM10 is $28.71 \mu\text{g}/\text{m}^3$. (Fig. 9) shows that the concentration of PM10 in Abu Dhabi ranges between Good ($0-50 \mu\text{g}/\text{m}^3$ year) which cover 0.01% of the city area as a mean annual, and between Very unhealthy ($200 - 300 \mu\text{g}/\text{m}^3$ year) which cover 0.02%, while unhealthy for sensitive groups ($100-150 \mu\text{g}/\text{m}^3$ year) cover 64.11%, Moderate ($50-100 \mu\text{g}/\text{m}^3$ year) 35.38% and unhealthy ($150 - 200 \mu\text{g}/\text{m}^3$ year) cover 0.048% of the city area. The Hudayriat Island developed districts in the east and northwest, as well as those near the industrial sectors in the west, are those that have experienced the most damage.

4.2.6. Muscat: Muscat is the best among the GCC countries capitals in PM10 concentration, with a mean annual of $71.32 \mu\text{g}/\text{m}^3$, this may be due to its large area, as mountains and deserts cover 78.1%, this placed it into the Moderate air ($50-100 \mu\text{g}/\text{m}^3$ year). PM10 mean annual concentration ranged between $328.94 \mu\text{g}/\text{m}^3$ as a maximum value and $40.65 \mu\text{g}/\text{m}^3$ as a minimum, as this average reached $78.79 \mu\text{g}/\text{m}^3$ in Summer and $71.64 \mu\text{g}/\text{m}^3$ in spring, while it reached $65.5 \mu\text{g}/\text{m}^3$ in winter. The main sources of PM10 high concentration are industrial emissions, through the combustion of coal, diesel, and natural gas as well as the extraction of other materials such as crude oil as major contributors. In addition to other elements including dust and super finely ground sand particles being blown into the city, along with construction sites and vehicle emissions forming up most majority of these monitored observation. (Fig. 10) shows that the concentration of PM10 in Muscat ranges between Good ($0-50 \mu\text{g}/\text{m}^3$ year) which cover 1.36% of the city area as a mean annual Which exceeded that in winter and autumn and reaching 9.41-4.52 respectively, and between very

unhealthy (200 -300 $\mu\text{g}/\text{m}^3$ year) which cover 0.01%, while Moderate (50–100 $\mu\text{g}/\text{m}^3$ year) cover 97.66%, unhealthy for sensitive groups (100–150 $\mu\text{g}/\text{m}^3$ year) cover 0.94%, and unhealthy (150 -200 $\mu\text{g}/\text{m}^3$ year) cover 0.03% of the city area. The southern districts near industrial regions (Rusayl, Ghala, and Bawshar) and the northern districts next to Muscat International Airport are the most susceptible.

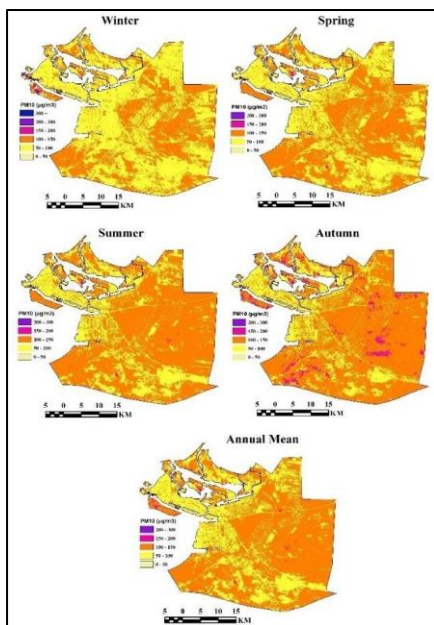


Fig. (9) Concentration of PM10 in Abu Dhabi

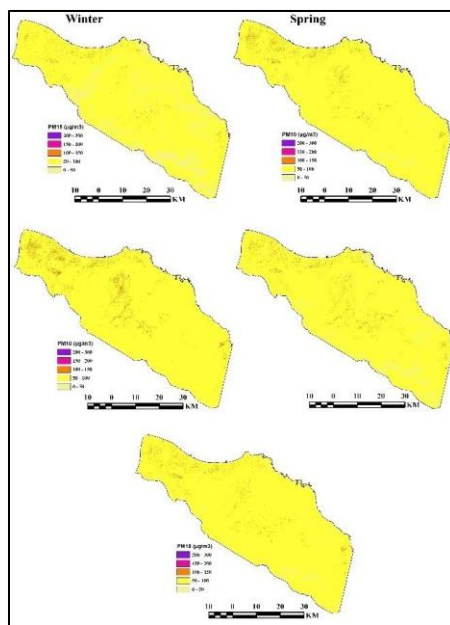


Fig. (10) Concentration of PM10 in Muscat

4.3. Air Quality Index Map of (GCC) capitals:

The Air Quality Index (AQI), created by the US Environmental Protection Agency (EPA), measures the amount of air pollution. The Air Quality Index typically has an impact on the five major air pollutants: ground level ozone, particulate matter, carbon monoxide, sulphur dioxide, and nitrogen dioxide. The measured pollutant concentration is given a number between zero and five hundred, with the range from good to extremely unhealthy. Greater AQI values indicate higher levels of air pollution and, consequently, worse general health. The AQI is proportional to air pollution.

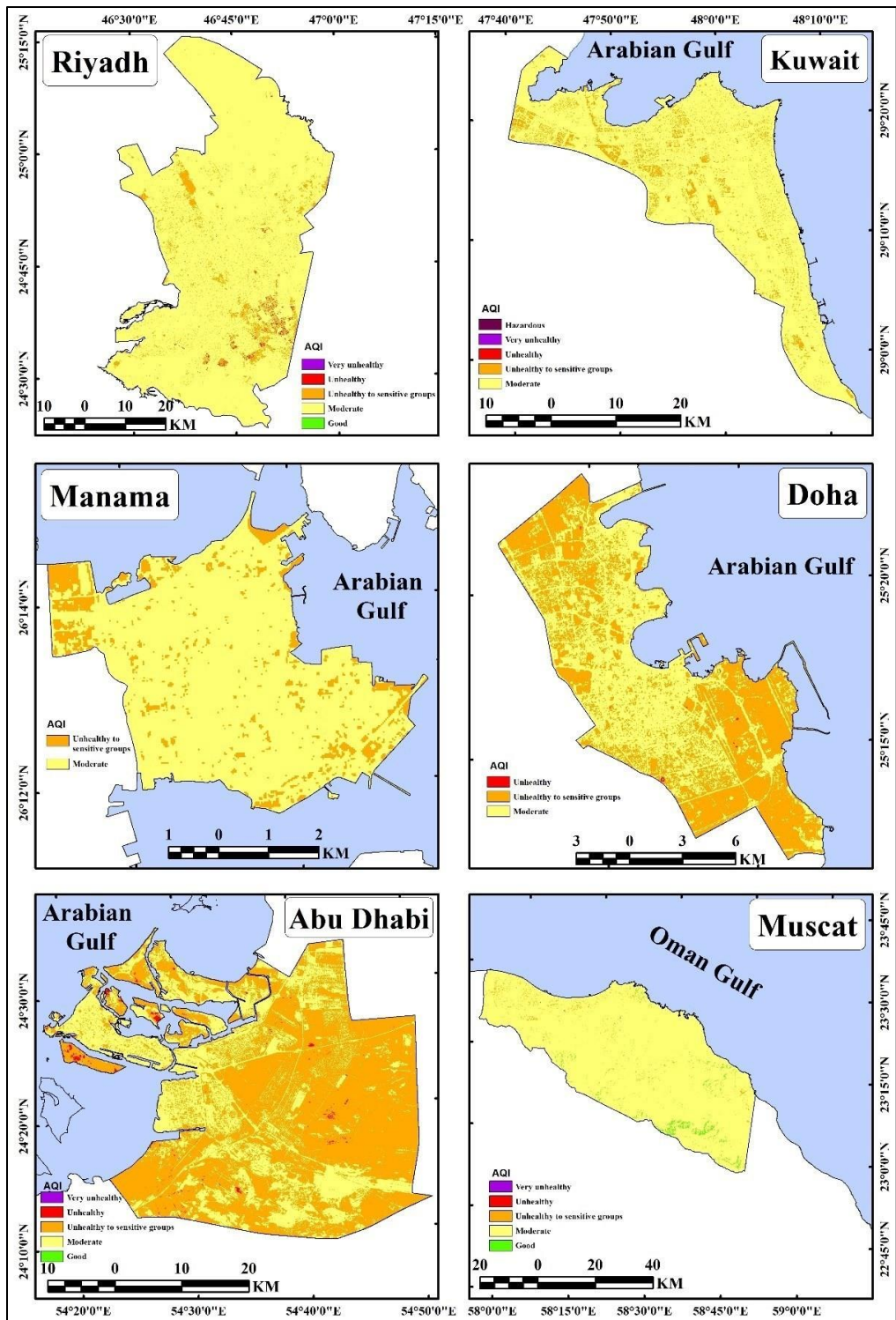


Fig. (11) Mean Annual AQI in GCC capitals 2021

Table 3 Mean Annual AQI in GCC capitals 2021

City	Winter	Spring	Summer	Autumn	Ave.
Riyadh	118	126	123	124	123
Kuwait	130	125	142	131	132
Manama	123	139	134	125	130
Doha	149	160	154	156	154
Abu Dhabi	147	156	164	183	162
Muscat	84	96	111	92	96
Ave.	125	134	138	135	133

To calculate air quality index, the study depended upon concentration of PM10 extracted from Landsat 8(OLI_TIRS) images, as index were calculated using the mean annual concentration of PM10 for the (GCC) capitals. (Fig. 11) and (table 3) reveal that the general mean annual of air quality index in (GCC) Capitals reached 133 therefore thesis cities are in the moderate category except Abu Dhabi and Doha, Where the mean annual reached (154-162) respectively, and therefore are in the category of unhealthy for sensitive groups. The most notable matters are that:

4.3.1. Riyadh: low air quality index areas are concentrated in the southern margin of the city where industrial areas affected air quality in addition to some parts in the middle of the city with intense population as well as northeastern due to intense human activities. These areas cover about 5.62% off the city area. Otherwise, the remaining parts of the city are in the moderate air quality category covering about 94.37% of the city area.

4.3.2. Kuwait: areas with low air quality are concentrated in northwestern and southeastern parts of the city, where industrial areas and petroleum refiners are located. In addition to some parts in the middle of the city due to high population density. These regions cover about 9.1% of the city area, while moderate air quality region cover about 90.9% of the city area. Regions with good air quality never appear.

4.3.3. Manama: region with low air quality cover 11.35% of the city area, these areas locate in the southern parts of the city where industrial areas are located, and in the northwest part due to intense human

activities. Whereas region with moderate air quality cover about 88.65% of the city area, Regions with good air quality never appear.

4.3.4. Doha: regions with low air quality cover 49.36% of the city area, these areas are distributed in two sections, the first is in the south where industrial region and Hamad international airport are located. The second section is in the north west where districts with high population density (ie Khalifa city, Al Duhail and umm Salal) region with moderate air quality index cover about 50.64%. there is no evidence of areas with good air quality.

4.3.5. Abu Dhabi: regions with low air quality are cover most parts of the city especially southern and eastern parts which witness high development rates resulting in continuously bursting and dusts, in addition to Hudayriat Island. These areas cover about 64.61% of the city area, whereas areas with moderate air quality cover 35.38% appear in the northeastern.

4.3.6. Muscat: low air quality cover 0.98% of the city area and appear in the northern and western parts of the city, due to over population in the north and industrial region in the west. Moderate air quality areas cover 97.66%, good air quality appear in the mountain area, south Muscat state and parts of Qurayyat and Al Amirat provinces, covering 1.36%.

5. Conclusion:

To estimate the PM10 concentration over (GCC) capitals, Landsat-8 (OLI_TIRS) was used. Based on an aerosol optical reflectance model, the PM10 algorithm is used. The results indicate that a PM10 model can extract and estimate air pollution with a high degree of accuracy based on the visible bands reflectance value. In order to address the considerable shortage of data observation, enhance data coverage, and improve data comparability, the project aims to model, monitor, and observe air quality in the Gulf Cooperation Council (GCC). This is done by integrating numerous datasets (such as Landsat-8 images, GIS technology).

The study concluded that PM10 concentrations are moderate in (GCC) capitals and above WHO air quality limits by a factor of two. Due to the local dusty air, it is most intense in the summer and autumn. According to the AQI, 76.25% of the capitals of the Gulf Cooperation Council have moderate air quality (AQI: 51-100).

Reference:

- Al-Khadouri, A., Al-Yahyai, S., Charabi, Y., (2015): *Contribution of atmospheric processes to the degradation of air quality: case study (Sohar Industrial Area, Oman)*. Arab. J. Geosci. 8 (3):1623 –1633. <https://doi.org/10.1007/s12517-014-1295-0>.
- Brown, K.W., Bouhamra, W., Lamoureux, D.P., Evans, J.S., Koutrakis, P., (2008): *Characterization of particulate matter for three sites in Kuwait*. J. Air Waste Manage. Assoc. 58 (8): 994 – 1003. <https://doi.org/10.3155/1047-3289.58.8.994>.
- EAD, (2013): *Enhancing Air Quality in Abu Dhabi*. 2014.pdf, Accessed date: 24 April 2018.
- El-Mubarak, A.H., Rushdi, A.I., Al-Mutlaq, K.F., Bazeyad, A.Y., Simonich, S.L., Simoneit, B.R., (2014): *Identification and source apportionment of polycyclic aromatic hydrocarbons in ambient air particulate matter of Riyadh, Saudi Arabia*. Environ. Sci. Pollut. Res. 21 (1):558 –567. <https://doi.org/10.1007/s11356-013-1946-9>.
- Engelbrecht, J.P., McDonald, E.V., Gillies, J.A., Jayanty, R.K.M., Casuccio, G., Gertler, A.W., (2009): *Characterizing mineral dusts and other aerosols from the Middle East—part 1: ambient sampling*. Inhal. Toxicol. 21 (4):297 –326. <https://doi.org/10.1080/08958370802464299>.
- Ettouney, R.S., Zaki, J.G., El-Rifai, M.A., Ettouney, H.M., (2010): *An assessment of the air pollution data from two monitoring stations in Kuwait*. Toxicol. Environ. Chem. 92 (4): 655 –668. <https://doi.org/10.1080/02772240903008609>.
- Hassan, R., Rahman, M., Hamdan, A., (2022): *Assessment of air quality index (AQI) in Riyadh, Saudi Arabia*, IOP Conf. Series: Earth and Environmental Science 1026 (2022) 01200. doi:10.1088/1755- 1315/1026/1/012003.
- Khamdan, S.A.A., Al-Madany, I.M., Buhussain, E., (2009): *Temporal and spatial variations of the quality of ambient air in the Kingdom of Bahrain during 2007*. Environ. Monit. Assess. 154 (1 – 4):241 –252. <https://doi.org/10.1007/s10661-008-0392-5>.
- Mishra R, Pandey J, Chaudhary S, Khalkho A, Singh V (2013): *Estimation of air pollution concentration over Jharia coalfield*

- based on satellite imagery of atmospheric aerosol, International Journal of Geomatics and Geosciences, Volume 4, No 1, p.30.*
- *Moawad, B, M., Youssief, A, A., Madkour, K., (2017): Modeling and Monitoring of Air Quality in Greater Cairo Region, Egypt Using Landsat-8 Images, HYSPLIT and GIS Based Analysis, Climate Change Research at Universities pp 37–54. DOI 10.1007/978-3-319-58214-6_3.*
 - *Moran, M., Jackson, R., Slater. P., and Teillet, P., (1992): Evaluation of simplified procedures for retrieval of Land surface reflectance factors from satellite sensor output. Remote Sensing of Environment, 41, 169-184*
 - *Morand, C., Maesano,I., (2004): Air pollution: from sources of emissions to health effects, Breathe | December 2004 | Volume 1 | No 2, p109.*
 - *Nadzri O, Mohd ZMJ, Lim HS (2010): Estimating Particulate Matter Concentration over Arid Region Using Satellite Remote Sensing: A Case Study in Makkah, Saudi Arabia. Modern Applied Science 4: 131-142. DOI:10.5539/mas.v4n11p131.*
 - *Nawahda, A., (2015): Monitoring the temporal variations of PM2.5 and gases close to the highway in Sohar, Oman. Int. J. Environ. Stud. 72 (4):685 –695. <https://doi.org/10.1080/00207233.2015.1057963>.*
 - *Nguyen, N, H., Tran, V, A., (2014): Estimation of PM10 from AOT of satellite Landsat image over Hanoi city, International Symposium on Geoinformatics for Spatial Infrastructure Development in Earth and Allied Sciences.*
 - *Omidvarborna, H., Baawain, M., Al-Mamun., (2018): Ambient air quality and exposure assessment study of the Gulf Cooperation Council countries: A critical review, Science of the Total Environment 636 (2018) 437 –448. <https://doi.org/10.1016/j.scitotenv.2018.04.296>.*
 - *Othman, N., Mat Jafri, M., Lim, H., Abdullah, K., (2009): Retrieval of Aerosol Optical Thickness (AOT) and its Relationship to Air Pollution Particulate Matter (PM10), Sixth International Conference on Computer Graphics, Imaging and Visualization,*

DOI 10.1109/CGIV.2009.22.

- Ramadan, A.A., (2010): *Air quality assessment in southern Kuwait using diffusive passive samplers. Environ. Monit. Assess. 160 (1 – 4):413 –423. <https://doi.org/10.1007/s10661-008-0705-8>.*
- Raouf, M., (2008): *Climate change threats, opportunities, and the GCC countries. The Middle East Institute Policy Brief. 12: pp. 1 – 15 (Last access on December 2016).*
- Retalis A, Sifakis N (2010): *Urban aerosol mapping over Athens using the differential textural analysis (DTA) algorithm on MERIS - ENVISAT data, ISPRS Journal of Photogrammetry and Remote Sensing, 65: 17–25. <https://doi.org/10.1016/j.isprsjprs.2009.08.001>.*
- Saleh SAH, Hasan G, (2014): *Estimation of PM10 Concentration using Ground Measurements and Landsat 8 OLI Satellite Image. J Geophys Remote Sens 3: 120. <http://dx.doi.org/10.4172/2169-0049.1000120>.*
- Saraswat, I., Mishra, R, K., Kumar, M., (2017): *Estimation of PM10 concentration from Landsat 8 OLI satellite imagery over Delhi, India, Remote Sensing Applications: Society and Environment 8 (2017) 251–257. <http://dx.doi.org/10.1016/j.rsase.2017.10.006>.*
- Sikder, S., Islam, A, M., (2018): *Aerosol Optical Thickness (AOT) Assessment Using GIS & Remote Sensing, International Journal of Innovative Research in Computer Science & Technology (IJIRCST) ISSN: 2347-5552, Volume-6, Issue-4, July 2018 DOI: 10.21276/ijircst.2018.6.4.5.*
- U.S. Geological Survey, (2020): *Landsat 8 Collection 1 (C1) Land Surface Reflectance Code (LaSRC) Product Guide.*
- Van, T., Nguyen, H., Bao, V., Bao, H., (2018): *Remote Sensing-Based Aerosol Optical Thickness for Monitoring Particular Matter over the City, Proceedings 2018, 2, 362; doi:10.3390/ecrs-2-05175.*
- Yahi, H., Santer, R., Weill, A., Crepon, M., Thiria, S., (2011): *Exploratory Study for Estimating Atmospheric Low Level Particle Pollution Based on Vertical Integrated Optical Measurements, Atmospheric Environment, 2011, p. 448. <https://doi.org/10.1016/j.atmosenv.2010.11.047>.*